Electronic Supplementary Material (ESI) for Journal of Materials Chemistry
This journal is © The Royal Society of Chemistry 2012

Supporting information for

Controlled synthesis of shell cross-linked magnetic micelles for efficient liver MR imaging

Dechao Niu,[a] Zhiwen Zhang,[b] Shijun Jiang,[b] Zhi Ma,[c] Xiaohang Liu,[d] Yongsheng Li,*[a] Liangping Zhou,[d] Changsheng Liu,[a] Yaping Li,*[b] and Jianlin Shi*[a,e]

[a] *School of Materials Science and Engineering, East China University of Science and Technology, Shanghai 200237, China.*

[b] *Center of Pharmaceutics, Shanghai Institute of Materia Medica, Chinese Academy of Sciences, Shanghai 201203, China*

[c] *Shanghai Institute of Organic Chemistry, Chinese Academy of Sciences, Shanghai 200032, China*

[d] *Department of radiology, Shanghai Cancer hospital, Fudan University, Shanghai, 200032, China*

[e] *State Key Laboratory of High Performance Ceramics and Superfine Microstructure, Shanghai Institute of Ceramics, Chinese Academy of Sciences, Shanghai 200050, China*

This journal is © The Royal Society of Chemistry 2012

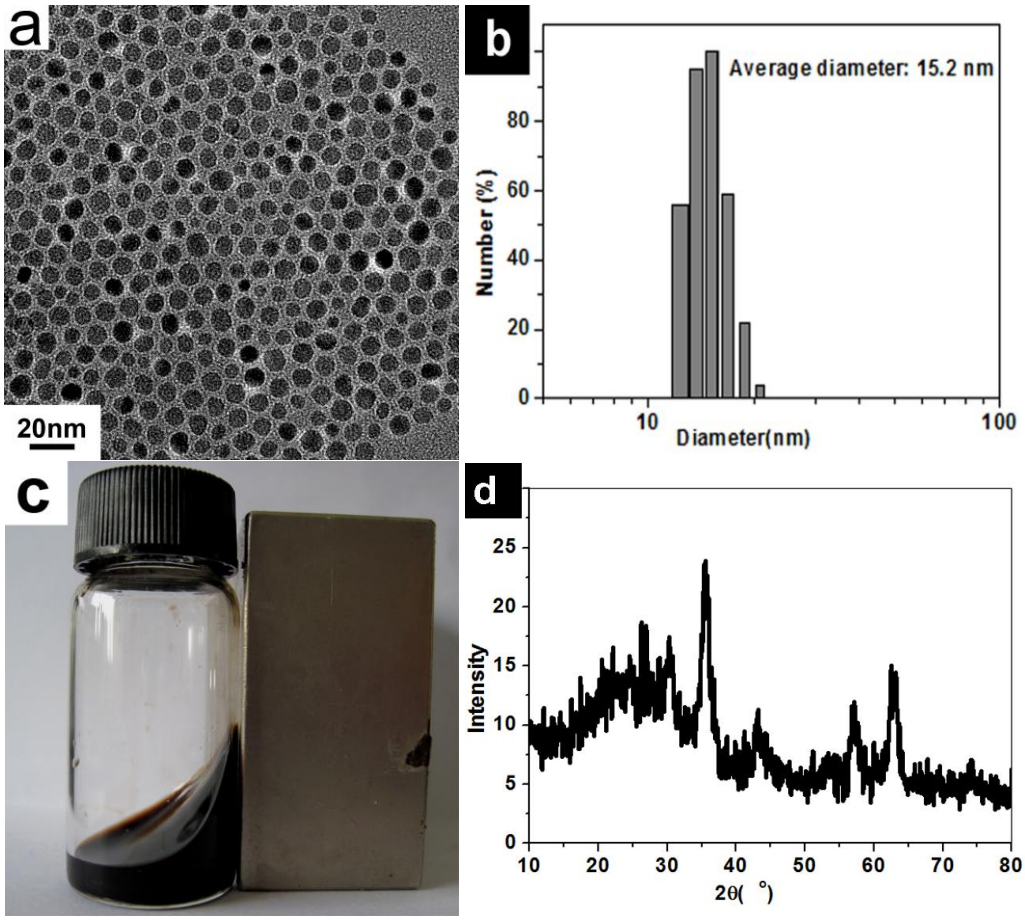

Figure S1. (a) TEM image and (b) particle size distribution of hydrophobic magnetite nanoparticles determined by dynamic light scattering (DLS) measurements in THF; (c) Photograph of magnetically attracted Fe_3O_4 nanoparticles dispersed in THF; (d) XRD pattern of 6 nm magnetite nanoparticles.

This journal is © The Royal Society of Chemistry 2012

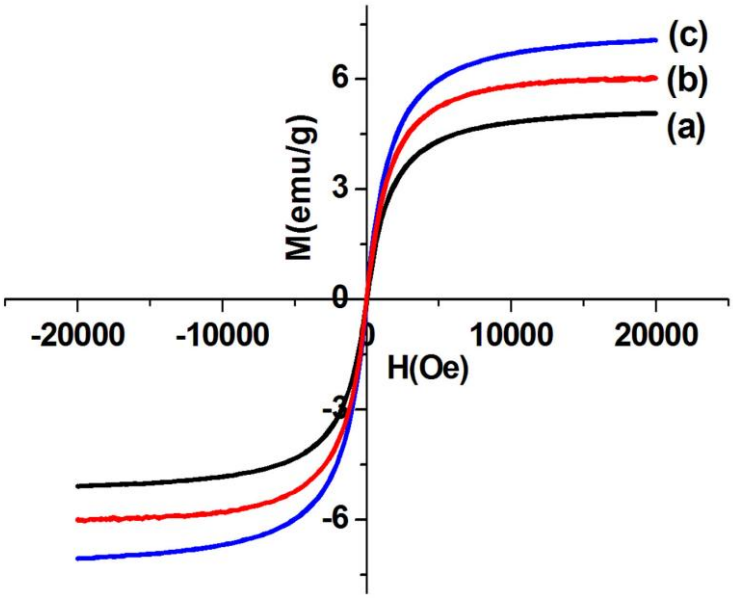

Figure S2. Field-dependent magnetization hysteresis loop of RhB-SCL-MMs-80 (a), RhB-SCL-MMs-130 (b) and RhB-SCL-MMs-180 (c) at 300 K.

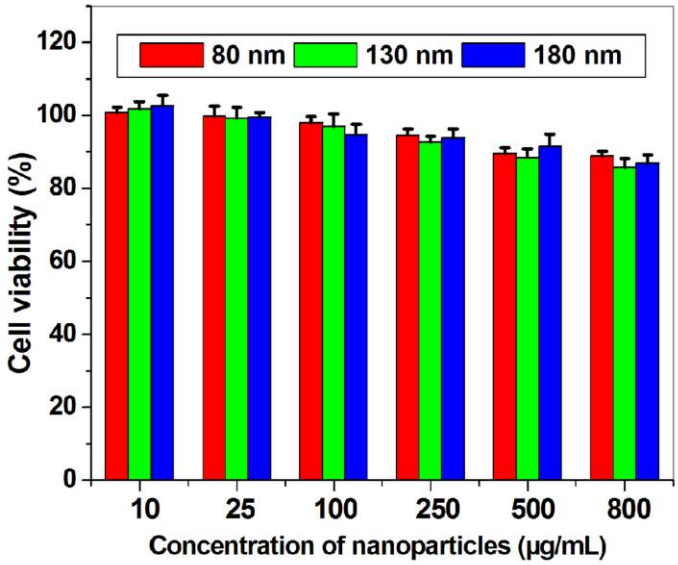

Figure S3. Cell viability of macrophage cell line RAW264.7 treated with various concentrations of RhB-SCL-MMs-80, RhB-SCL-MMs-130 and RhB-SCL-MMs-180 as measured by the MTT assay.

This journal is © The Royal Society of Chemistry 2012

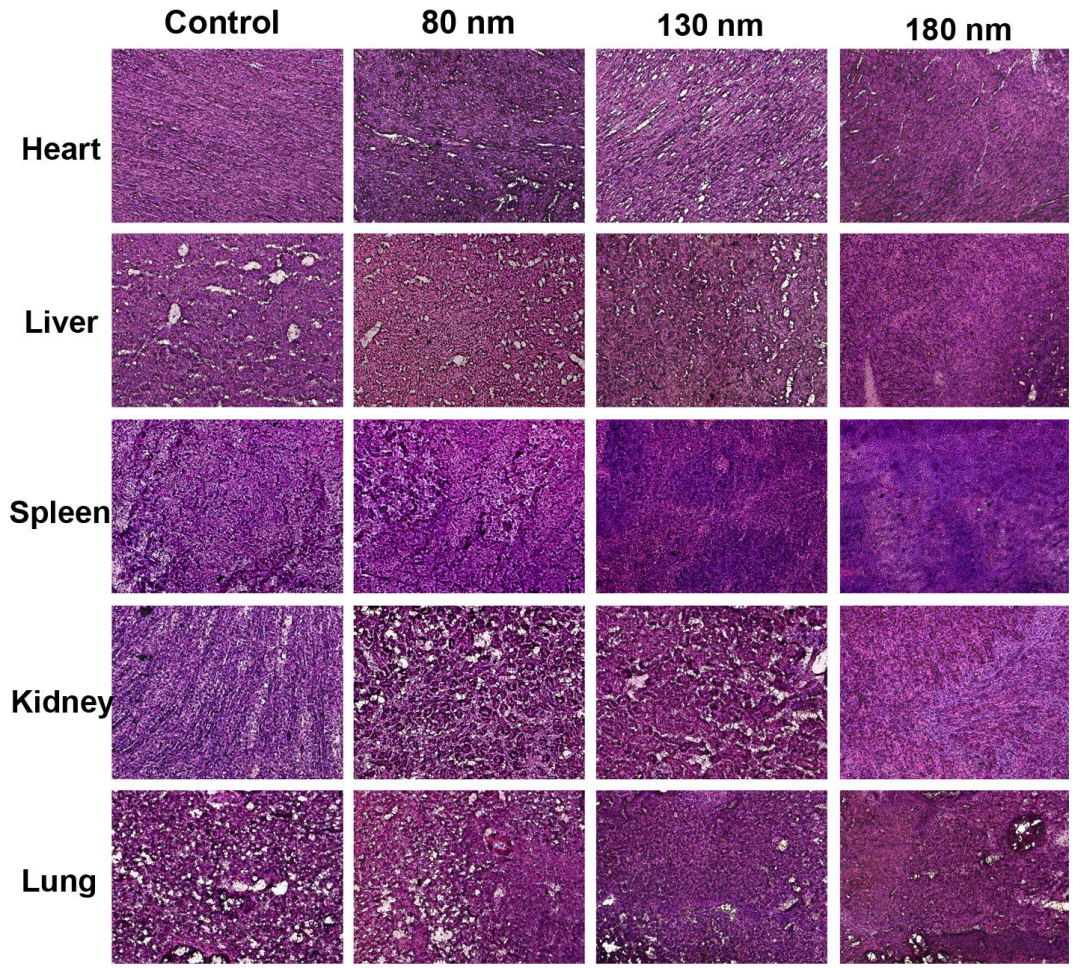

Figure S4. Histological analysis of heart, liver, spleen, kidney, and lung tissue from ICR mice in 24 h of injection with RhB-SCL-MMs-80, RhB-SCL-MMs-130 and RhB-SCL-MMs-180 through tail veins. Images were acquired at 100× magnification.

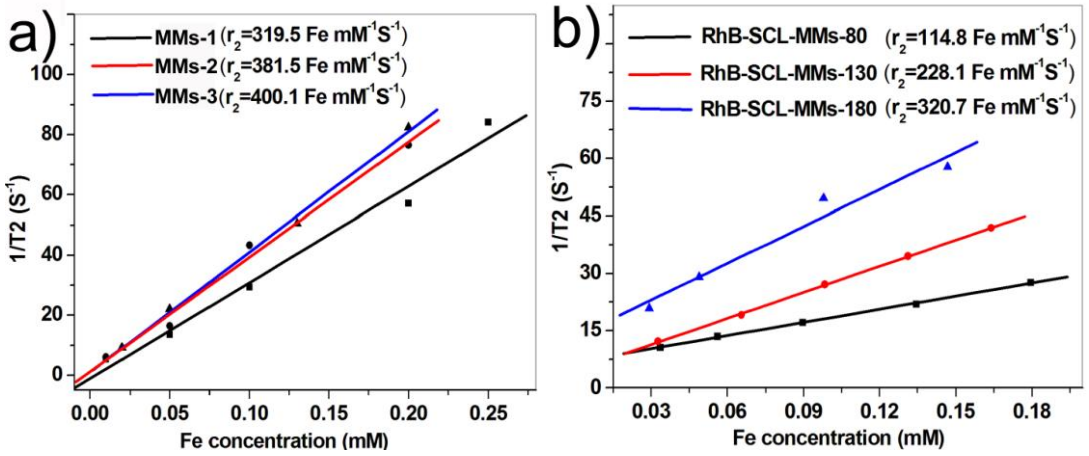

Figure S5. T_2 relaxation rate ($1/T_2$) as a function of Fe concentration for the MMs (a) and the RhB-SCL-MMs (b) at 3.0 T, respectively. The slope indicates the specific relaxivity value, r_2.

This journal is © The Royal Society of Chemistry 2012

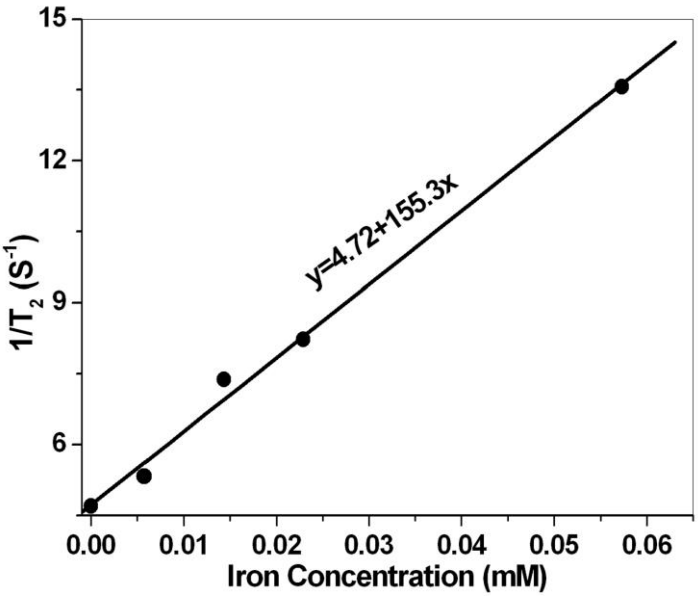

Figure S6. T_2 relaxation rate ($1/T_2$) as a function of Fe concentration for the DMSA-coated Fe_3O_4 containing single magnetite nanoparticles at 3.0 T, which were synthesized based on the reported method [ref 11 in the text]. Y. M. Huh, Y. W. Jun, H. T. Song, S. Kim, J. S. Choi, J. H. Lee, S. Yoon, K. S. Kim, J. S. Shin, J. S. Suh, J. Cheon, *J. Am. Chem. Soc.* **2005,** *127*, 12387.

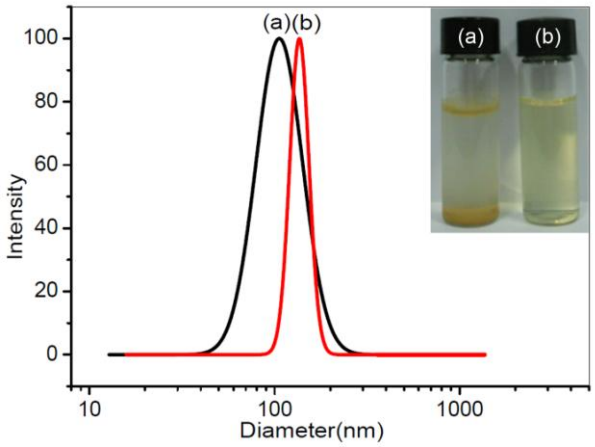

Figure S7. Hydrodynamic diameters of SCL-MMs in water (a) and PEGylated SCL-MMs in PBS (b) determined by DLS. The inset is digital photograph of samples dispersed in PBS. The results show that the diameter of SCL-MMs increased from 110.7 to 137.2 nm after PEGylation, indicating the successful grafting of PEG molecules on the surface of SCL-MMs. Besides, the PEGylated SCL-MMs displays well stability in PBS, while the SCL-MMs without PEG precipitated quickly in PBS solution. This phenomenon further confirmed the important role of PEG in biomedical applications.